Luminescence of crystals excited by a runaway electron beam and by excilamp radiation with a peak wavelength of 222 nm

D. A. Sorokin, A. G. Burachenko, D. V. Beloplotov, V. F. Tarasenko, E. Kh. Baksht, E. I. Lipatov, and M. I. Lomaev

Citation: Journal of Applied Physics **122**, 154902 (2017);

View online: https://doi.org/10.1063/1.4996965

View Table of Contents: http://aip.scitation.org/toc/jap/122/15

Published by the American Institute of Physics

Luminescence of crystals excited by a runaway electron beam and by excilamp radiation with a peak wavelength of 222 nm

D. A. Sorokin,[1,2,a)] A. G. Burachenko,[1] D. V. Beloplotov,[1,2] V. F. Tarasenko,[1,2] E. Kh. Baksht,[1] E. I. Lipatov,[1] and M. I. Lomaev[1,2]
[1]*Institute of High Current Electronics, 2/3 Akademichesky Ave., Tomsk 634055, Russia*
[2]*National Research Tomsk State University, 36 Lenin Ave., Tomsk 634050, Russia*

(Received 20 July 2017; accepted 6 October 2017; published online 20 October 2017)

This paper presents research data on cathodoluminescence, photoluminescence, and Cherenkov radiation at 200–800 nm excited in crystals with different refractive indices by a subnanosecond runaway electron beam and by KrCl excilamp radiation with a peak wavelength of 222 nm. The data include spectral and amplitude-time characteristics measured with a resolution of up to ~100 ps for natural and synthetic diamonds of type IIa, sapphire, CsI, ZnS, CaF_2, ZrO_2, Ga_2O_3, $CaCO_3$, CdS, and ZnSe. The research suggests that cathodoluminescence and photoluminescence should be accounted for in Cherenkov-type detectors of runaway electrons. The results can be useful for detecting high-energy electrons in tokamaks. *Published by AIP Publishing.*
https://doi.org/10.1063/1.4996965

I. INTRODUCTION

Runaway electrons (RAEs) can adversely affect plasma heating in controlled thermonuclear research systems.[1,2] Although this fact is well-known from theory, no reliable detectors of such electrons are available. Recent research on tokamaks has focused much attention on RAEs[3–8] as fast electrons add to the loss of energy and to the evaporation of vacuum chamber walls. Different types of devices are developed to detect high-energy electrons, and most widely used in tokamaks are Cherenkov-type detectors.[9–11] Such detectors, as a rule, comprise a diamond which is shielded with a metal film against plasma and from which visible and UV radiation produced by RAEs is recorded with a photomultiplier tube connected to the detector via a quartz fiber. The design of Cherenkov-type detectors is constantly improved, allowing one to obtain more reliable data on the generation of RAEs during plasma heating.[10,11] Unfortunately, no paper is available comparing the parameters of Cherenkov radiation and cathodoluminescence excited in diamonds by RAEs or presenting RAE energy spectra.

Cherenkov radiation, which is well known from theory[12] and experiments, can be emitted by liquids, gases, and solids when charged particles, e.g., electrons, move in them with velocities higher than the phase velocity of light, and its intensity can increase up to a certain limit both with decreasing wavelength λ and with increasing kinetic electron energy ε. This type of radiation arises at a certain energy threshold ε_{thr} which depends on the refractive index n and decreases with increasing n. For diamond, ε_{thr} is ~50 keV.[9–11] This crystal is used for recording Cherenkov radiation due to its UV transparency up to 223 nm, high heat conductivity and heat resistance, and high electrical conductivity on electron beam excitation.

Some papers[13–15] report that in natural and synthetic diamonds and in other crystals, the radiation at 200–800 nm excited by a pulsed electron beam of energy from several tens to several hundreds of kiloelectronvolts is mainly due to cathodoluminescence; in particular, this is observed for a subnanosecond electron beam[15] known as a supershort avalanche electron beam (SAEB).[16–18] Note that in RAE-excited polymethyl methacrylate, Cherenkov radiation escapes detection.[19]

Here, we present research data on the spectral and amplitude-time characteristics of radiation excited in crystals with high refractive indices by RAE beams of different densities and durations and by pulsed KrCl excilamp radiation with a peak wavelength of 222 nm.

II. POWER OF CHERENKOV RADIATION

The power spectral density of Cherenkov radiation $dJ(\lambda)/d\lambda$ for kinetic electron energy ε can be expressed in terms of effective radiative deceleration F[12]

$$VdF = dJ(\lambda) = 4\pi^2 e^2 V\left(1 - \frac{c^2}{V^2 n^2}\right)\frac{d\lambda}{\lambda^3}, \tag{1}$$

$$\frac{V}{c} = \frac{\sqrt{(1+\varepsilon/mc^2)^2 - 1}}{1+\varepsilon/mc^2}. \tag{2}$$

Here, n is the refractive index of a medium, λ is the radiation wavelength, m is the electron mass, V is the electron velocity, and c is the velocity of light in vacuum. The threshold energy ε_{thr} for Cherenkov radiation to arise is estimated from the condition that the bracketed term in the right-hand side of (1) is equal to zero. For example, for diamond with $n = 2.42$, $\varepsilon_{thr} = 50$ keV. Figure 1 shows curves calculated by the above expressions for Cherenkov radiation. From the n dependence of ε_{thr} [Fig. 1(a)], it is seen that the lower the refractive index n, the higher the threshold energy ε_{thr} for Cherenkov radiation.

a)Author to whom correspondence should be addressed: SDmA-70@loi.hcei.tsc.ru

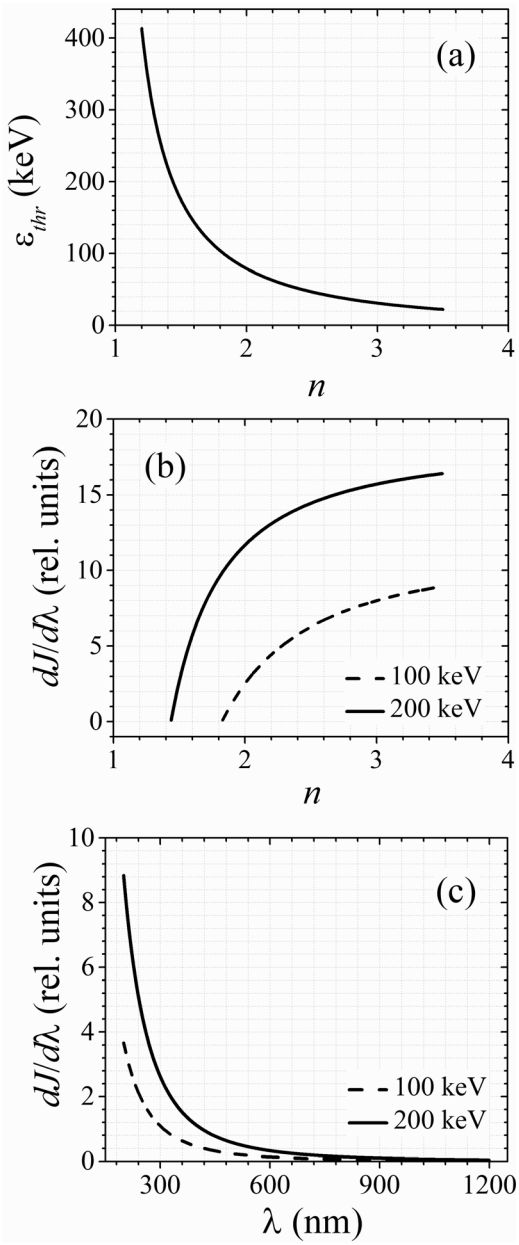

FIG. 1. Calculated curves for Cherenkov radiation: threshold electron energy ε_{thr} vs. refractive index n (a), power spectral density $dJ/d\lambda$ vs. n at $\lambda = 200$ nm (b), and $dJ/d\lambda$ vs. λ (c) in diamond excited by electrons at 100 and 200 keV.

The n dependence of the power spectral density $dJ/d\lambda$ at $\lambda = 200$ nm for different electron energies [Fig. 1(b)] suggests that increasing the refractive index n not only decreases the threshold ε_{thr} for Cherenkov radiation but also provides a several-fold increase in its spectral energy density at the same electron energy. Thus, crystals with $n \geq 2.42$ should be used to obtain Cherenkov radiation at $\varepsilon \leq 50$ keV.

What is of importance is that for all materials studied, the power spectral density of Cherenkov radiation $dJ/d\lambda$ increases with both decreasing λ (up to the fundamental absorption edge) and increasing ε. Thus, using UV- and VUV-transparent crystals, we can separate the radiation in these spectral regions from cathodoluminescence. Such behavior of Cherenkov radiation can be seen on the diagrams for diamond at 100 and 200 keV [Fig. 1(c)] although they are in the spectral region of low absorption for the material.

III. PROPERTIES OF CRYSTALS

Several types of crystals (Table I) were exposed to a SAEB and UV radiation.

The highest values of n among them belong to diamonds, ZnSe, CdS, ZnS, and ZrO_2. However, CdS and ZnS are unsuitable for Cherenkov-type detectors because of their sufficient transmittance only at >500 nm, and CaF_2 and Al_2O_3 (sapphire), although transparent to both UV and vacuum ultraviolet (VUV), have low values of n as do CsI and $CaCO_3$. Note that crystals for high-energy electron detectors should also display high heat conductivity and thermal stability.

Most suited for detectors of runaway electrons are diamonds. Although they were used in tokamaks,[9–11] no comparison has been made between the intensities of cathodoluminescence and Cherenkov radiation for them and other crystals. In Sec. VI, we present data on the spectral and amplitude-time characteristics of radiation for different crystals.

IV. EXPERIMENTAL SETUP AND TECHNIQUES

The crystals were exposed to SAEBs produced in accelerators based on gas-filled diodes[15–19] using a GIN-55–01 generator[20] and a RADAN-220 generator.[21]

The GIN-55–01 generator produced voltage pulses of amplitude 110 kV with a rise time of ≈0.7 ns and a FWHM of ≈1 ns at a resistive load of >1 kΩ. The pulse repetition frequency f could be varied from one to 100 Hz. The spectral characteristics of the crystals were measured at $f = 65$ Hz. The FWHM τ_b of the SAEB current and its density j_b were ~100 ps and ~1.6 A/cm^2, respectively. The average electron beam energy was 60 keV. Downstream of the anode foil, the number of electrons with an energy greater than ε_{thr} for diamond (≈50 keV) was >60%.

The RADAN-220 generator was operated at a pulse repetition frequency of 1 Hz and provided the generation of a SAEB in two modes[22] depending on the gas kind and pressure. In mode #1, the SAEB parameters were $j_b \approx 75$ A/cm^2

TABLE I. Bandwidth B_w, refractive index n, and threshold electron energy ε_{thr} for different crystals.

Crystal type \ Characteristic	B_w (μm)	n	ε_{thr} (keV)
Natural diamond, IIa type	0.225–5	2.42	50
Synthetic diamond, IIa type	0.225–5	2.42	50
ZnSe	0.475–20	2.4	51
CdS	0.52–1	2.4	51
ZnS	0.37–13.5	2.2	63
ZrO_2	0.35–7	2.158	65
Ga_2O_3	0.26–1	1.97	82
Al_2O_3 (sapphire)	0.18–2.3	1.77	108
CsI	0.3–35	1.74	113
$CaCO_3$	0.25–1	1.57	152
CaF_2	0.125–12	1.434	202

and $\tau_b \approx 180$ ps, and in mode #2, they were $j_b \approx 1$ A/cm^2 and $\tau_b \approx 100$ ps. In both modes, the percent of beam electrons with an energy of >50 keV was greater than 95%. The electron energy distribution showed two maxima at ≈80 and ≈150 keV. It should be noted that of all the electrons downstream of the anode foil, the percent of those with an energy of >200 keV was less than 1%.

For the crystals excited by a runaway electron beam, we measured both the spectrum of cathodoluminescence and the spectrum of Cherenkov radiation in the short-wavelength range.

The crystals were also excited by a KrCl excilamp[23] with a peak wavelength of 222 nm. Its average radiation power density was 7 mW/cm^2. The FWHM of radiation pulses produced by the excilamp at $f = 43$ kHz was 200 ns. The crystals were shaped as disks and were irradiated from the side of their flat surface with recording of luminescence at their lateral surface. Thus, it was possible to greatly reduce the fraction of visible radiation emitted by the barrier discharge plasma. On excitation by the excilamp, there was no cathodoluminescence or Cherenkov radiation. Thus, when using the excilamp only, photoluminescence was registered.

The emission and transmission spectra of the crystals were recorded with a HR2000 + ES spectrometer of known spectral sensitivity (an instrumental function, FWHM ~9 Å). The spectral range of the spectrometer was $\Delta\lambda = 190$–1100 nm. Figure 2 shows a schematic of the experimental setup for research in the radiation properties of crystals. The use of a quartz fiber greatly reduced the level of electromagnetic noise in spectral measurements.

The results of spectral measurements of crystal radiation are presented in units of the spectral energy density $\rho(\lambda)$.

The amplitude-time characteristics of radiation in narrow spectral ranges were studied using a LOMO MDR-23 monochromator with a groove density of the grating of 1200 gr/mm and an inverse linear dispersion of 1.3 nm/mm. The width of its entrance and exit slits was 400 μm. The monochromator was equipped with a Hamamatsu H7732–10 photomultiplier tube of known spectral sensitivity (sensitivity range, 10^3–10^7 and rise time, 2.2 ns). The spectral range of the photomultiplier was $\Delta\lambda = 185$–900 nm.

The amplitude-time characteristics of radiation at 200–700 nm were also investigated using a Photek PD025 photodiode equipped with a LNS20 photocathode. The transient response rise time of the photodiode was ~80 ps. The short-wavelength boundary of radiation was determined by crystal absorption and its long-wavelength boundary by decreased photodiode sensitivity. Because no fiber was used for radiation transfer to the photodiode, it was possible, unlike elsewhere,[15] to detect radiation in a spectral region of up to 200 nm.

The runaway electron beam parameters were measured using a collector with the diameter of the receiving of 20 mm.[15,16]

The signals from the photodiode and collector were transmitted to a Keysight Tech DSO-X 6004A digital oscilloscope (6 GHz, 20 GS/s) and the signals from the photomultiplier to a Tektronix TDS3054B digital oscilloscope (500 MHz, 5 GS/s).

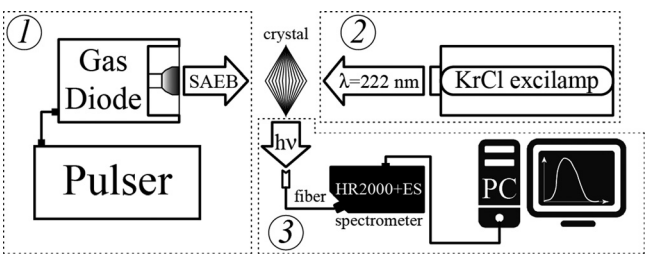

FIG. 2. Schematic of the experimental setup. *1*—excitation by SAEB, *2*—excitation by KrCl excilamp radiation, and *3*—measuring system.

V. RESULTS AND DISCUSSION

A. Emission spectra of crystals

The cathodoluminescence that arises on exposure to a SAEB was measured for eleven crystals differing in refraction and transmission: natural and synthetic diamonds of type IIa, CsI, ZnS, Al_2O_3, CaF_2, ZrO_2, Ga_2O_3, CdS, ZnSe, and $CaCO_3$. The Cherenkov radiation intensity was low and undetectable against the background of cathodoluminescence, which agrees with data reported elsewhere.[13–15] Figures 3–5 present emission spectra for the crystals excited by a SAEB (curves *1* and *2*). Additionally, the figures show transmission spectra (curves *4*) and photoluminescence bands for some crystals on their excilamp excitation (curves *3*); the radiation intensity is given in relative units. The presented curves illustrate the spectral distribution of radiation energies. Note that

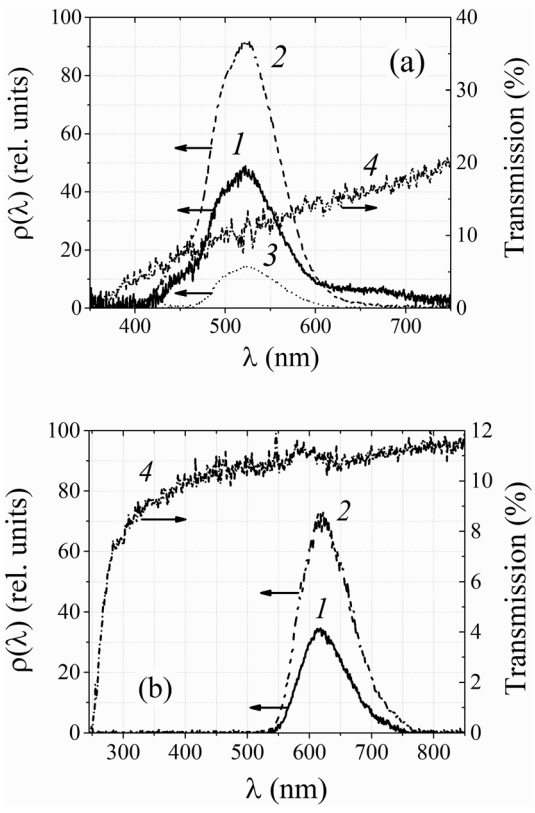

FIG. 3. Emission (*1–3*) and transmission spectra (*4*) of ZnS (a) and $CaCO_3$ (b) excited by SAEB on the GIN-55-01 generator (*1*) and RADAN-220 generator in mode #1 (*2*) and by radiation of KrCl excilamp (*3*).

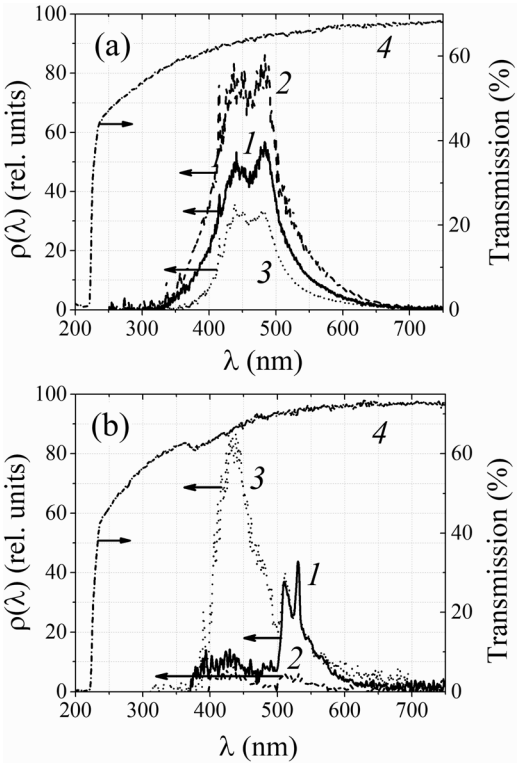

FIG. 4. Emission (*1–3*) and transmission spectra (*4*) of natural (a) and synthetic diamonds (b) excited by SAEB on the GIN-55-01 generator (*1*) and RADAN-220 generator in mode #1 (*2*) and by radiation of KrCl excilamp (*3*).

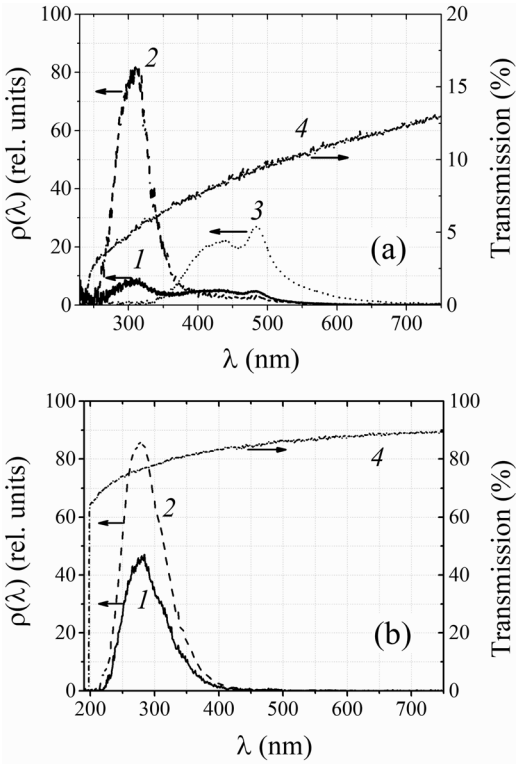

FIG. 5. Emission (*1–3*) and transmission spectra (*4*) of CsI (a) and CaF_2 (b) excited by SAEB on the GIN-55-01 generator (*1*) and RADAN-220 generator in mode #1 (*2*) and by radiation of KrCl excilamp (*3*).

from these data, it is impossible to judge the intensity ratio for different radiation types in a single excitation pulse. The radiation intensities in the crystals excited using the GIN-55–01 generator, RADAN-220 generator, and excilamp differed greatly.

The spectrograms of ZnS and $CaCO_3$ (Fig. 3), as well as of natural and synthetic diamonds (Fig. 4), reveal a large region between the absorption and emission edges where the desired signal is indistinguishable against the noise. The same is observed for Ga_2O_3. From Fig. 5(a), it is seen that for CsI, the edges of short-wavelength absorption and cathodoluminescence are almost coincident, making it difficult to detect Cherenkov radiation in this spectral region. For CaF_2, the edge of short-wavelength absorption lies in the VUV region [Fig. 5(b)], but the edge of its luminescence band does reach 225 nm.

The cathodoluminescence intensity in Figs. 4(a) and 4(b) is given in relative units. Comparison of its absolute values for natural and synthetic diamonds suggests that the cathodoluminescence intensity in natural diamond is an order of magnitude greater than that in synthetic. The emission spectrum for synthetic diamond excited by a SAEB in the repetitive pulsed mode contains intense bands at 500–550 nm [Fig. 4(b), spectrum *2*], while no such bands are found in the emission spectrum for natural diamond.

Thus, the presented emission spectra suggest the possibility of detecting Cherenkov radiation, in particular in synthetic diamond, using more sensitive methods.

Photoluminescence was detected for natural and synthetic diamonds, CsI, ZnS, ZrO_2, and Ga_2O_3 excited by excilamp radiation and was not detected for sapphire and CaF_2 due to their low absorption at 200–250 nm. No photoluminescence was also observed for CdS, ZnSe, and $CaCO_3$.

The data on excitation by the KrCl excilamp demonstrate that short-wavelength radiation contributes to photoluminescence, the bands of which coincide with those of cathodoluminescence for most of the crystals. It can also be concluded that the cathodoluminescence and photoluminescence bands for most of the crystals are similar. For synthetic diamond excited by the excilamp in the repetitive pulsed mode, the photoemission spectrum also reveals intense bands at 500–550 nm [Fig. 4(b), spectrum *3*].

Thus, photoluminescence can be contributed by Cherenkov radiation whose intensity increases with decreasing λ [Fig. 1(c)] and possibly by its part in the range of increasing crystal absorption.

B. Amplitude-time characteristics of crystal radiation

The photodiode used to measure the amplitude-time characteristics of radiation on SAEB excitation provided subnanosecond time resolution but low sensitivity. The photomultiplier at the monochromator output had high sensitivity and allowed us to detect low-intensity radiation in narrow spectral ranges at a time resolution of no worse than 2 ns.

Figure 6 shows the cathodoluminescence power for synthetic diamond excited by a SAEB with a FWHM of 100 ps. The radiation pulse has a FWHM of ~2 ns and a rise time of ~1 ns. The data confirm that the radiation is contributed mostly by cathodoluminescence. The time resolution of the measuring system with the photodiode was no worse than

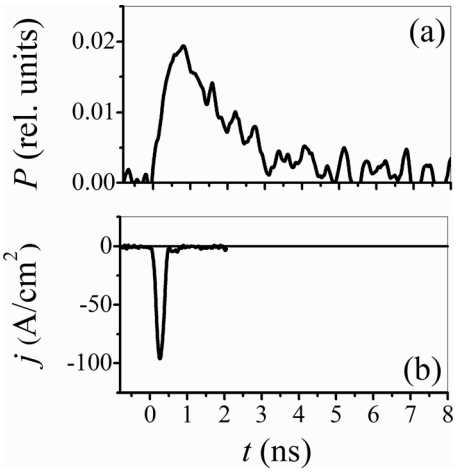

FIG. 6. Cathodoluminescence power (a) and SAEB current density (b) of synthetic diamond.

0.3 ns and corresponded to the radiation pulse rise time in $CaCO_3$ on SAEB excitation.

As noted above, the spectral range between the edges of short-wavelength absorption and cathodoluminescence is most suitable for the detection of Cherenkov radiation. Using the photomultiplier and monochromator, Cherenkov radiation was detected in natural and synthetic diamonds, ZnS, ZrO_2, Ga_2O_3, sapphire, and even in CsI. The sensitivity of the photomultiplier was sufficient to provide reliable measurements for these crystals. The absorption of CdS and ZnSe in the region shorter than 500 nm is high, and these crystals are thus unsuitable for Cherenkov-type detectors. Detecting Cherenkov radiation in CaF_2 and $CaCO_3$ requires their excitation by a beam with an electron energy higher than 200 keV.

Figure 7 shows the spectral energy density $\rho(\lambda)$ as a function of the wavelength for natural (*1*) and synthetic diamonds (*2*) excited by a SAEB. The dependencies take into account the sensitivity of the photomultiplier and the spectral transmission of the measuring optical elements.

It is seen from Fig. 7 that for natural diamond at 230–310 nm and for synthetic diamond at 230–350 nm, $\rho(\lambda)$ increases with decreasing λ. The radiation pulse duration in these regions for the crystals remains constant and corresponds to the time resolution of the photomultiplier. The radiation pulses have no delay with respect to the voltage rise and can be considered as Cherenkov radiation. Starting with 310 nm for natural diamond and with 350 nm for synthetic diamond, the radiation power and the pulse duration increase several times with the increasing wavelength, which agrees with the data of Fig. 4.

The contribution of cathodoluminescence and Cherenkov radiation to the total emitted energy was estimated by joining the data of spectrometer and monochromator measurements with subsequent calculations of the Cherenkov radiation and cathodoluminescence energies. For natural and synthetic diamonds, the Cherenkov radiation energy was determined as $\int_{230}^{310}\rho(\lambda)d\lambda$ and $\int_{230}^{370}\rho(\lambda)d\lambda$, respectively. The integration limits were chosen from the data of Fig. 7. The cathodoluminescence energy for natural and synthetic diamonds was determined as $\int_{310}^{750}\rho(\lambda)d\lambda$ and $\int_{350}^{650}\rho(\lambda)d\lambda$, respectively (see Fig. 4). The estimation suggests that the Cherenkov radiation energy in the emission spectrum is ~0.1% for natural diamond and 10% for synthetic diamond.

Besides, there is a delay of cathodoluminescence with respect to Cherenkov radiation in this spectral range. According to measurements, the delay increases gradually to 4–5 ns (Fig. 8).

Similar delays and an increase in radiation pulse duration were detected by the photomultiplier for ZnS, ZrO_2, Ga_2O_3, Al_2O_3, and CsI in the region between edges of short-wavelength absorption and cathodoluminescence and in the region of cathodoluminescence as well. Hence, all these crystals can be used for detecting Cherenkov radiation but only with monochromators and highly sensitive photomultipliers.

C. Discussion

Our research shows that cathodoluminescence can greatly exceed Cherenkov radiation over a wide spectral range. It depends on the beam current density, electron energy, and pulse repetition frequency and can be used to create more sensitive detectors of runaway electrons.

Cherenkov radiation at electron energies of tens to hundreds of kiloelectron-volts was detected in natural and synthetic diamonds, ZnS, ZrO_2, Ga_2O_3, sapphire, and CsI. For detecting electrons with an energy of ~50 keV from Cherenkov radiation, one should use crystals with a refractive index of 2.4 and higher. It should also be kept in mind that Cherenkov radiation is the easiest to detect in the region

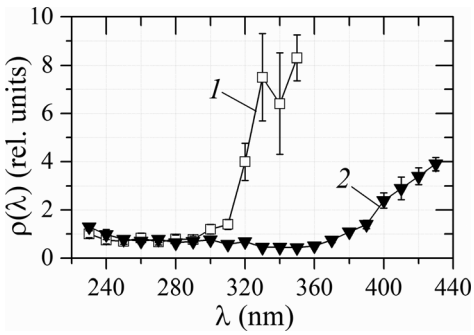

FIG. 7. Spectral energy density $\rho(\lambda)$ vs. wavelength for natural (*1*) and synthetic diamonds (*2*) excited by SAEB in mode #2, measured with the MDR-23 monochromator and photomultiplier.

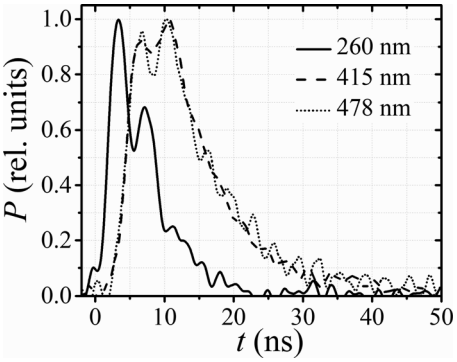

FIG. 8. Radiation power at 260, 415, and 478 nm, measured with a photomultiplier at monochromator output. RADAN-220 generator: mode #2.

between the edges of short-wavelength absorption and cathodoluminescence. For the crystals used, no other intense emission bands should be present in the spectrum.

The percent of Cherenkov radiation on excitation by electron beams with energies of tens to hundreds of kiloelectronvolts is ~0.1% for natural diamond and 10% for synthetic diamond. The physical and optical properties of synthetic diamonds with a small impurity amount make them most suitable for Cherenkov-type detectors; in our experiments, it was an IIa-type synthetic diamond grown by chemical vapor deposition. The main advantage of Cherenkov radiation for use in runaway electron detectors is that it arises with zero delay. However, cathodoluminescence should be allowed for in creating this type of detectors.

Although it has been reported on the design of Cherenkov-type detectors,[9–11] no data are available on photomultiplier measurements of optical radiation for them. No data are also available on runaway electron energy spectra in tokamaks. It is expected that the research data presented here will be helpful for calibration of this type of detectors. Promising for this purpose are accelerators based on gas-filled diodes, which provide the generation of runaway electron beams with a current density of up to hundreds of amperes per square centimeter and with their energy, duration, and density variable by varying the diode pressure and generator voltage.[22,24]

When designing this type of detectors, one should take into account additional bands arising at 500–550 nm in the repetitive pulsed mode. Such bands appear in the emission spectrum of synthetic diamond excited by both runaway electrons and excilamp radiation. For some crystals, photoluminescence is likely to contribute to the total radiation due to short-wavelength absorption of Cherenkov radiation.

VI. CONCLUSION

Thus, we have investigated the optical properties of different crystals excited by runaway electron beams generated in accelerators based on gas-filled diodes and by radiation produced in a KrCl excilamp with a wavelength of 222 nm. The research data, including spectral and amplitude-time characteristics measured at 200–800 nm with subnanosecond resolution, show that runaway electron detectors should be designed with regard to cathodoluminescence and additional bands arising in crystals on repetitive pulsed excitation. It is expected that the research data will help to create and calibrate reliable high-energy electron detectors for tokamak systems.

ACKNOWLEDGMENTS

This work was performed under State Assignment for IHCE SB RAS (Project No. #9.5.2).

[1]R. Jayakumar, H. H. Fleischmann, and S. J. Zweben, Phys. Lett. A **172**, 447 (1993).
[2]M. N. Rosenbluth and S. V. Putvinski, Nucl. Fusion **37**, 1355 (1997).
[3]M. R. Ghanbari, M. Ghoranneviss, A. S. Elahi, S. Mohammadi, and R. Arvin, J. Fusion Energy **35**, 180 (2016).
[4]B. Pourshahab, M. R. Abdi, A. Sadighzadeh, and C. Rasouli, Phys. Plasmas **23**, 072501 (2016).
[5]Z. Popovic, B. Esposito, J. R. Martin-Solis, W. Bin, P. Buratti, D. Carnevale, and M. Riva, Phys. Plasmas **23**, 122501 (2016).
[6]Z. H. Jiang, X. H. Wang, Z. Y. Chen, D. W. Huang, X. F. Sun, T. Xu, and G. Zhuang, Nucl. Fusion **56**, 092012 (2016).
[7]L. Zeng, Z. Y. Chen, Y. B. Dong, H. R. Koslowski, Y. Liang, Y. P. Zhang, H. D. Zhuang, D. W. Huang, and X. Gao, Nucl. Fusion **57**, 046001 (2017).
[8]P. Aleynikov and B. N. Breizman, Nucl. Fusion **57**, 046009 (2017).
[9]V. V. Plyusnin, L. Jakubowski, J. Zebrowski, H. Fernandes, C. Silva, K. Malinowski, P. Duarte, M. Rabinsky, and M. J. Sadowski, Rev. Sci. Instrum. **79**, 10F505 (2008).
[10]L. Jakubowski, M. J. Sadowski, J. Zebrowski, M. Rabinsky, K. Malinowski, R. Mirowski, P. Lotte, L. Gunn, J. Y. Pascal, G. Colledany, V. Basiuk, M. Goniche, and M. Lipa, Rev. Sci. Instrum. **81**, 013504 (2010).
[11]L. Jakubowski, M. J. Sadowski, J. Zebrowski, M. Rabinsky, M. J. Jakubowski, K. Malinowski, R. Mirowski, P. Lotte, M. Goniche, L. Gunn, G. Colledani, J. Y. Pascal, and V. Basiuk, Rev. Sci. Instrum. **84**, 016107 (2013).
[12]L. D. Landau, J. S. Bell, M. J. Kearsley, L. P. Pitaevskii, E. M. Lifshitz, and J. B. Sykes, *Electrodynamics of Continuous Media* (Pergamon Press Ltd., 1984).
[13]V. I. Solomonov and S. G. Mikhailov, *Pulse Cathodoluminescence and Its Application for Analysis of Condensed Matter* (Ural Branch of RAS, Ekaterinburg, 2003) (in Russian).
[14]A. M. Zaitsev, *Optical Properties of Diamond: A Data Handbook* (Springer-Verlag, Berlin, 2001).
[15]E. K. Baksht, A. G. Burachenko, and V. F. Tarasenko, Tech. Phys. Lett. **36**, 1020 (2010).
[16]T. Shao, V. F. Tarasenko, C. Zhang, E. K. Baksht, D. Zhang, M. V. Erofeev, C. Ren, Y. V. Shutko, and P. Yan, J. Appl. Phys. **113**, 093301 (2013).
[17]D. Levko, Y. E. Krasik, V. F. Tarasenko, D. V. Rybka, and A. G. Byrachenko, J. Appl. Phys. **113**, 196101 (2013).
[18]V. F. Tarasenko, D. V. Rybka, A. G. Burachenko, M. I. Lomaev, and E. V. Balzovsky, Rev. Sci. Instrum. **83**, 086106 (2012).
[19]V. F. Tarasenko, E. K. Baksht, A. G. Burachenko, D. V. Beloplotov, and A. V. Kozyrev, IEEE Trans. Plasma Sci. **45**(1), 76–84 (2017).
[20]V. M. Efanov, M. V. Efanov, A. V. Komashko, A. V. Kirilenko, P. M. Yarin, and S. V. Zazoulin, *Ultra-Wideband, Short Pulse Electromagnetics 9* (Springer, New York, 2010).
[21]F. Ya. Zagulov, A. S. Kotov, V. G. Shpak, Yu. Yu. Yurike, and M. I. Yalandin, Prib. Tekh. Eksp. **2**, 146 (1989) (in Russian).
[22]V. F. Tarasenko, E. K. Baksht, A. G. Burachenko, I. D. Kostyrya, M. I. Lomaev, and D. A. Sorokin, IEEE Trans. Plasma Sci. **38**, 2583 (2010).
[23]M. I. Lomaev, E. A. Sosnin, and V. F. Tarasenko, Chem. Eng. Technol. **39**, 39 (2016).
[24]*Generation of Runaway Electron Beams and X-Rays in High Pressure Gases: Techniques and Measurements*, edited by V. F. Tarasenko (Nova Science Publishers Inc., New York, 2016), Vol. 1.